

# **Supplemental Figures**

## Supplemental Figure Legends

**Supplement Figure S1.** MIDY mutant V(B18)A retains some ability to produce and release human insulin in  $\beta$ -cells. Recombinant myc-tagged human proinsulin WT or MIDY mutants were transiently expressed in Min6 (mouse)  $\beta$ -cells. At 24 h after transfection, the bathing medium was changed to fresh medium that was then collected for 24 h without additional stimulation, before cell lysis and analysis of both lysates (yellow bars) and media (blue bars) by human-specific insulin ELISA. Mean + s.d. from  $n = 3$  independent experiments; \*  $p < 0.05$  for secreted human insulin derived from proinsulin-V(B18)A compared to that from other MIDY mutants.

**Supplement Figure S2.** MIDY mutant proinsulins are predisposed to form disulfide-linked complexes. Min6 (mouse)  $\beta$ -cells were transiently transfected with human WT or MIDY mutant proinsulins and resolved by nonreducing and reducing SDS-PAGE, as in Fig. 5. Disulfide-linked dimer + trimer bands detected by immunoblotting of the nonreducing gels with anti-Myc or anti-human proinsulin were divided by the total proinsulin band intensity detected by immunoblotting on the reducing gels, and the predisposition to form disulfide-linked complexes was compared to that of WT proinsulin (first bar); error bars (s.d.) and significant  $p$ -values are indicated on the figure.

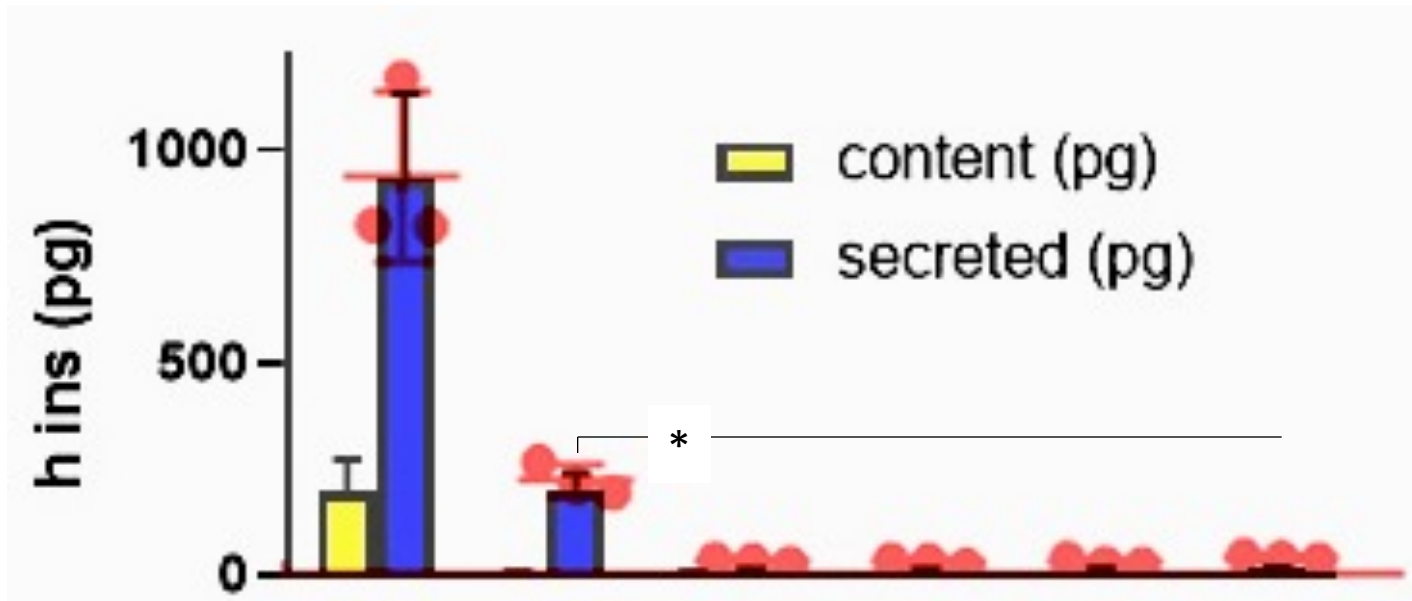
**Supplement Figure S3.** ER stress response measurement in  $\beta$ -cells expressing MIDY mutants. INS832/13  $\beta$ -cells were co-transfected with myc-tagged human WT or MIDY mutant proinsulins plus BiP-firefly luciferase and CMV-renilla luciferase. At 48 h post-transfection, luciferase activities in transfected cells were measured as described in Methods (mean  $\pm$  s.d.). As shown, all MIDY mutants showed a trend to increased ER stress, but only L(A16)P achieved statistical significance ( $p$ -value indicated on the figure) compared to WT proinsulin.

**Supplement Figure S4.** Oxidation of newly-synthesized proinsulin and lose-A6/A11 proinsulin. INS832/13  $\beta$ -cells were transfected to express myc-tagged human WT or MIDY mutant proinsulins (P), as well as WT or MIDY versions of lose-A6/A11 proinsulins (L). Pulse-labeling (without chase) and sample processing was performed as described in Figs. 4A and 6C, and the fastest-migrating (oxidized) forms were quantified (mean  $\pm$  s.d.) from at least 3 independent experiments. In the lose-A6/A11 background, the MIDY mutants H(B5)D and E(A4)K both exhibited significantly improved oxidative folding ( $p$ -values indicated on the figure). The third MIDY mutant whose secretion is increased in the lose-A6/A11 background, R(Cpep+2)C, already showed native-like disulfide bond formation even in the WT proinsulin background.

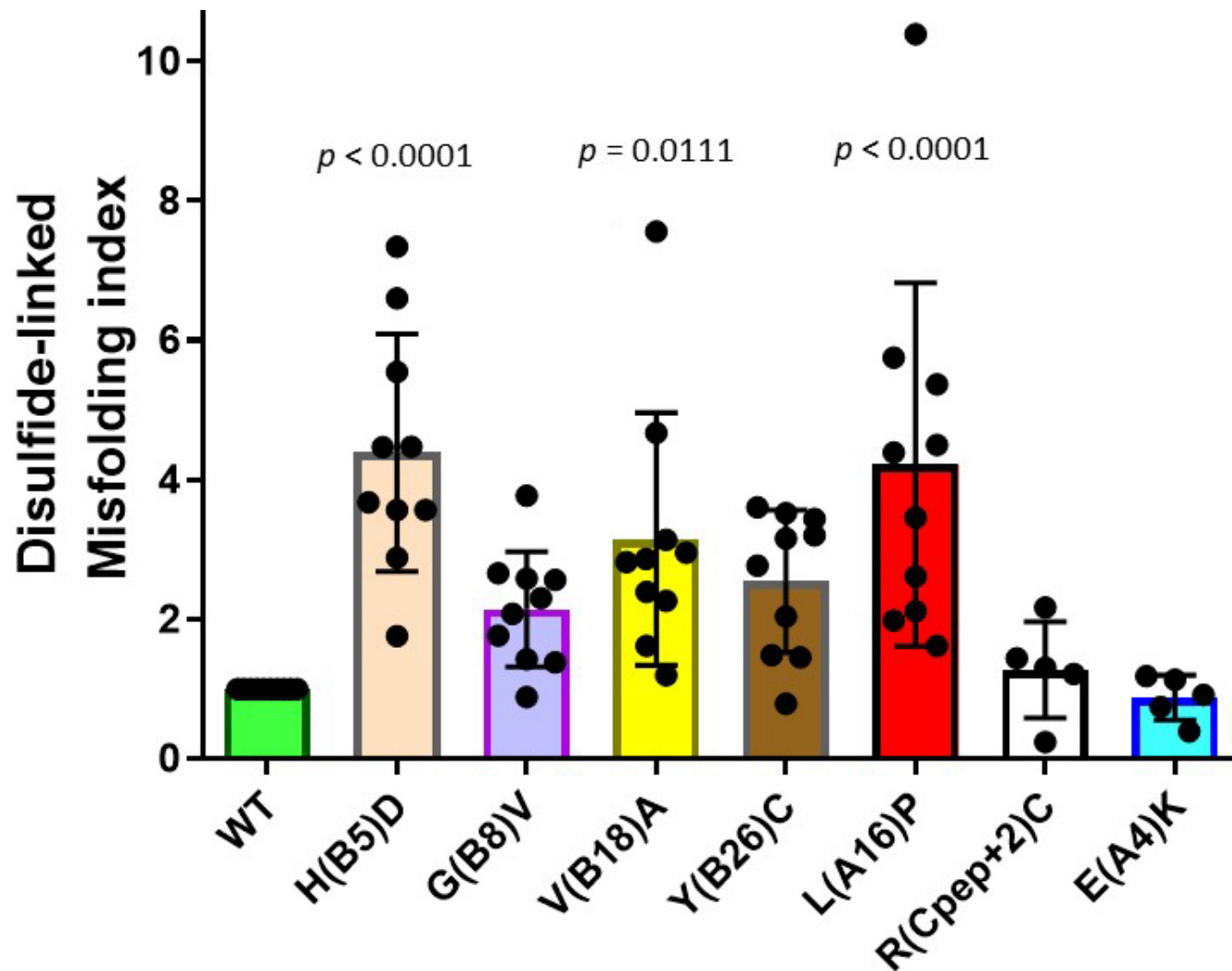
**Supplement Figure S5.** Live cell imaging of INS832/13 cells transiently expressing fluorescent WT or MIDY proinsulins (and their derived fluorescent protein products). The NIS Elements software “volume view” was used to create a 3D-tilt model to highlight the intracellular distribution of fluorescent protein. Top eight panels: WT or MIDY versions of hPro-CpepSfGFP (bearing superfolder-GFP embedded within the C-peptide). Only the WT construct displays a punctate fluorescence pattern typical of secretory granules in live  $\beta$ -cells (red box). Bottom eight panels: the same WT and MIDY hPro-CpepSfGFP constructs in the lose-A6/A11 background. In addition to WT, in this background E(A4)K, H(B5)D and R(Cpep+2)C all show a punctate fluorescence pattern typical of secretory granules in live  $\beta$ -cells (red boxes). The other constructs continued to show a fluorescence pattern typical of ER retention. The V(B18)A substitution was an exception showing a partial granule-like pattern, especially in the lose-A6/A11 background (yellow box). White scale bar = 10  $\mu$ m.

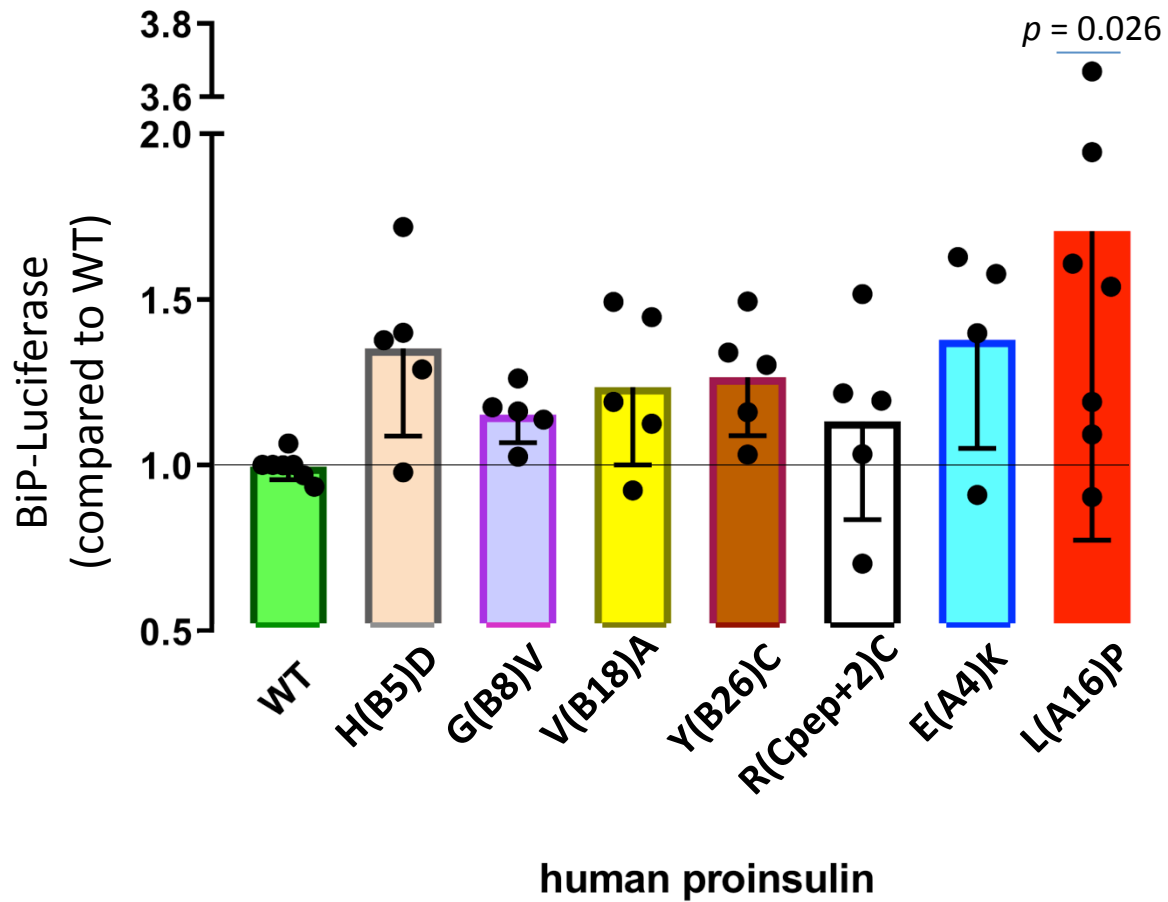
**Supplement Figure S6.** Oxidation and secretion of newly-synthesized lose-A6/A11 proinsulin bearing G(B8V) and G(B8)S MIDY substitutions. 293T cells transfected to express the indicated constructs were pulse-labeled with  $^{35}$ S-labeled amino acids, and both cell lysates and media were immunoprecipitated with guinea pig polyclonal anti-insulin at the indicated chase times. The samples were analyzed by Tris-tricine-urea-SDS-PAGE under nonreducing and reducing conditions, followed by autoradiography.

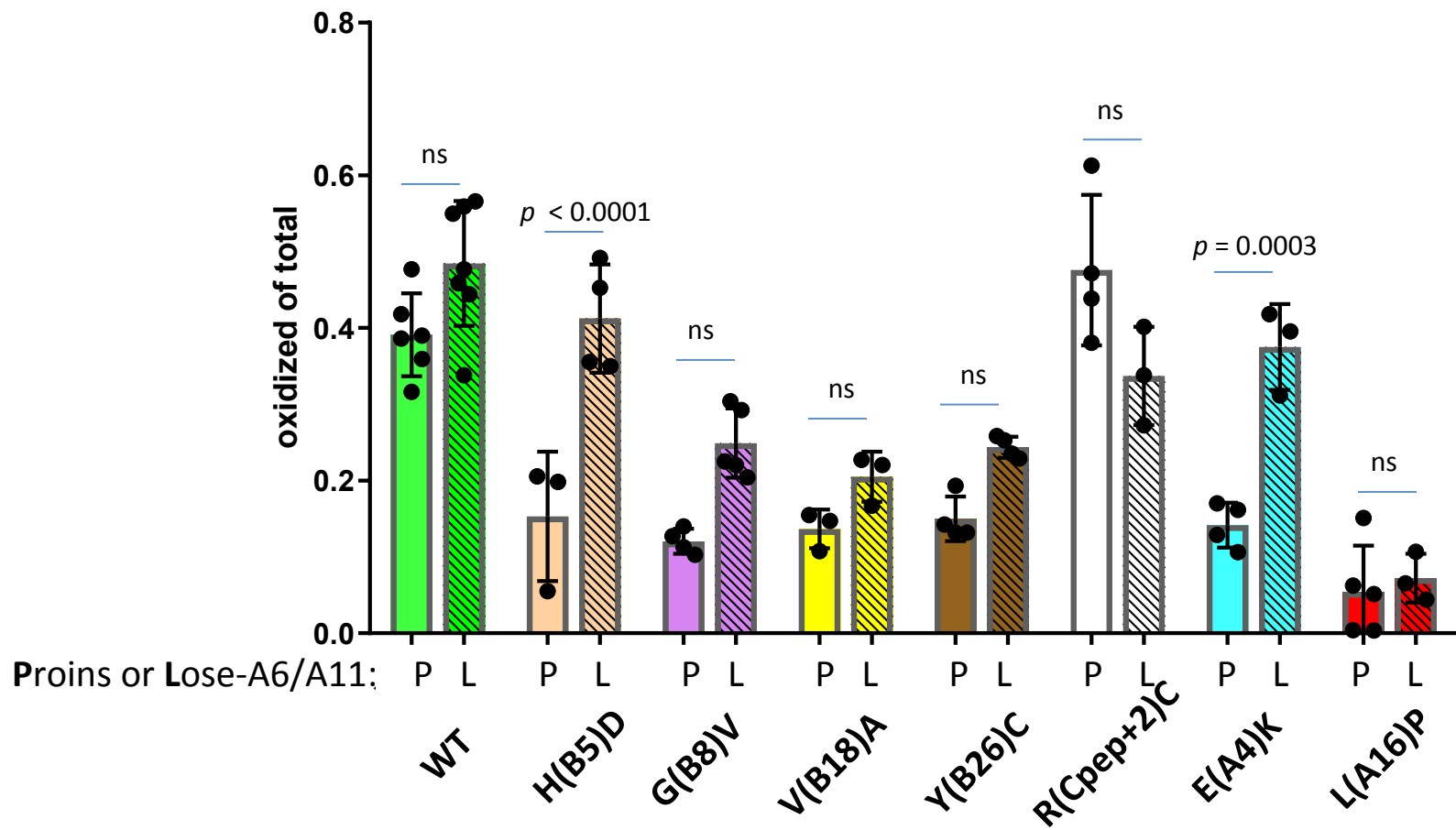
**Supplement Figure S7.** Structural environments of mutation sites in T-state insulin monomer (coordinates from Protein Databank entry 4INS; 2-Zn molecule-2). **A)** The imidazole side chain of H(B5) (blue dashed circle) packs within an inter-chain crevice near both the internal Cys(A6)-Cys(A11) disulfide bridge (these positions circled in the image) [and near Cys(A7) and Ser(A9) with which it forms bifurcating hydrogen bonds (dashed yellow lines)]. **B)** Packing of the side chain of Y(B26) within a shallow solvent-exposed inter-chain crevice lined by the side chains of F(B24), P(B28), G(A1) and I(A2). **C)** Internal side chain of L(A16) is shown in relation to insulin’s three  $\alpha$ -helices (ribbons, and a partially transparent protein surface). Core packing of L(A16) involves Cys(A6)-Cys(A11) (shown as yellow balls) and the side chains of L(B11), L(B15), I(A2), L(A13), and Y(A19); Cys(A20)-Cys(B19) (not shown) is also nearby. **D)** Packing of the side chain of V(B18) within a deep solvent-exposed interchain crevice lined by A(B14) and L(A13) at its lip and in its depths by the core side chains of L(A16) and Cys(A20).



Myc-tagged hProinsulin: WT V(B18)A Y(B26)C R(Cpep+2)C E(A4)K L(A16)P

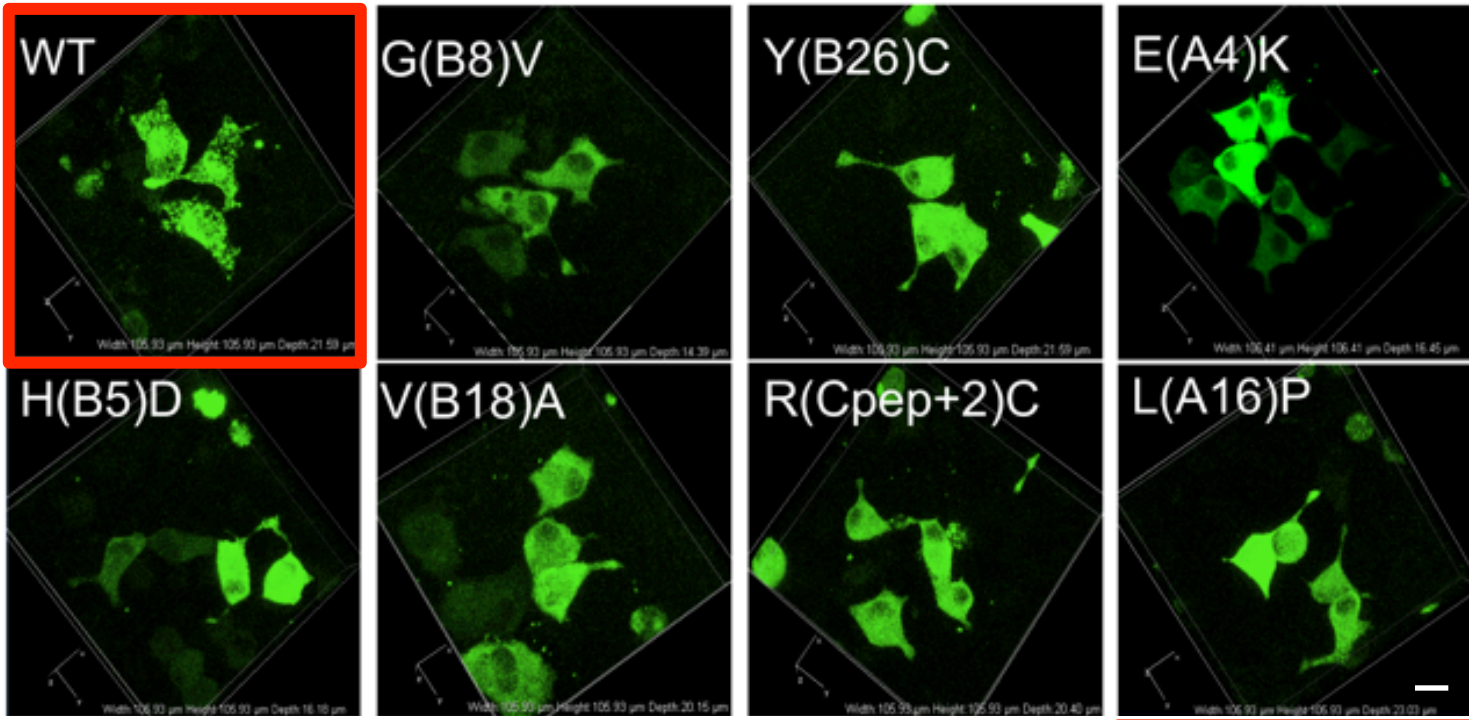






# hPro-CpepSfGFP

## Proinsulin



## LOSE-A6/A11

